



Available online at <http://scik.org>

Commun. Math. Biol. Neurosci. 2020, 2020:4

<https://doi.org/10.28919/cmbn/4069>

ISSN: 2052-2541

A FITTED OPERATOR METHOD FOR A MODEL ARISING IN VASCULAR TUMOR DYNAMICS

KOLADE M. OWOLABI*, KAILASH C. PATIDAR, ALBERT SHIKONGO

Department of Mathematics and Applied Mathematics, University of the Western Cape, Cape Town 7535, South Africa

Copyright © 2020 the author(s). This is an open access article distributed under the Creative Commons Attribution License, which permits unrestricted use, distribution, and reproduction in any medium, provided the original work is properly cited.

Abstract. In this paper, we consider a model for the population kinetics of human tumor cells in vitro, differentiated by phases of the cell division cycle and length of time within each phase. Since it is not easy to isolate the effects of cancer treatment on the cell cycle of human cancer lines, during the process of radiotherapy or chemotherapy, therefore, we include the spatial effects of cells in each phase and analyse the extended model. The extended model is not easy to solve analytically, because perturbation by cancer therapy causes the flow cytometric profile to change in relation to one another. Hence, making it difficult for the resulting model to be solved analytically. Thus, in [16] it is reported that the non-standard schemes are reliable and propagate sharp fronts accurately, even when the advection, reaction processes are highly dominant and the initial data are not smooth. As a result, we construct a fitted operator finite difference method (FOFDM) coupled with non-standard finite difference method (NSFDM) to solve the extended model. The FOFDM and NSFDM are analyzed for convergence and are seen that they are unconditionally stable and have the accuracy of $\mathcal{O}(\Delta t + (\Delta x)^2)$, where Δt and Δx denote time and space step-sizes, respectively. Some numerical results confirming theoretical observations are presented.

Keywords: cytometric dynamics; cell cycle; steady states; fitted operator method; stability analysis.

2010 AMS Subject Classification: 65M06.

*Corresponding author

E-mail address: mkowolax@yahoo.com

Received April 24, 2019

1. INTRODUCTION

It is a well known fact that vascular tumors are a highly diverse group of aberrant growths and they are relatively abundant in the human population, with infantile hemangiomas being the most common tumor in children and cavernous hemangiomas affecting approximately one in every one hundred people see [2] and the references therein. Thus, apart from our previous work reported in [18, 19, 20, 21] on tumors, we feel that it is essential for us as researchers to understand that genetic differences between people lead to differences in susceptibility. Since tumors develop in different organs and tissues of a body, then this should imply that a genetic heterogeneity among cancer cells, the cellular heterogeneity of the tumor tissue underlie a phenotype heterogeneity of the disease and cancer cells in a tumor are not all identical, but form different clones, defined as sets of cancer cells that share a common genotype [31]. Therefore, in our views, it is also very important to study dynamics for the kinetics of a population of cells differentiated by phases of the cell division cycle such as the ones presented by Jackiewicz et al., [12] as a way toward avoiding incorrect treatment decisions especially, if a biopsy sample is not representative of other parts of the tumor.

On the other hand, it is understood that even in the simplified environment of the laboratory with modern techniques and/or technology, it is not always possible to isolate the effects of cancer treatment on the cell cycle of human cancer cell lines. Therefore, it is important to mentioned some of the work done in the direction of understanding cancer cells from the cells cycle point of view. Thus, we highlight few work done in this direction of the studies. These are for instance Giotti et al., in [11] mentioned that cell division is central to the physiology and pathology of all eukaryotic organisms and in [4, 7, 8], have considered the in-vitro model of cancer therapies that target the cellular mechanisms of growth, division and death in all or some stages of the cell cycle. Thus, our first aim in this paper is to include the spatial distribution of each phase for the model derived in [4] and presented in [12]. The model in [12] is given as follow,

$$(1) \quad \left. \begin{aligned} \frac{\partial G_1(x,t)}{\partial t} &= 4bM(2x,t) - (k_1 + \mu_{G_1})G_1(x,t), \\ \frac{\partial S(x,t)}{\partial t} &= \varepsilon \frac{\partial^2 S(x,t)}{\partial x^2} - g \frac{\partial S(x,t)}{\partial x} - \mu_S S(x,t) + k_1 G_1(x,t) - I(x,t, T_S), \\ \frac{\partial G_2(x,t)}{\partial t} &= I(x,t; T_S) - (k_2 + \mu_{G_2})G_2(x,t), \\ \frac{\partial M(x,t)}{\partial t} &= k_2 G_2(x,t) - bM(x,t) - \mu_M M(x,t), \end{aligned} \right\}$$

where, $x, t \geq 0$, T_S , $G_1(x, t)$, $S(x, t)$, $G_2(x, t)$, $M(x, t)$, μ_{G_1} , μ_S , μ_{G_2} , and μ_M denote the dimensionless relative DNA content, time in hours, time in hours, density of cells in G_1 phase, density of cells in DNA synthesis or S phase, density of cells in G_2 phase and mitosis or M phase, death rates in G_1 , S , G_2 , and M phases, respectively. The parameters k_1 and k_2 denote the transition probabilities of cells from G_1 phases to S phase and from G_2 phases to M phase, respectively, $b, 0 < \varepsilon \lll 1, g \ggg 1$ denote division rate, dispersion coefficient and average growth rate of DNA in the S phase. The $4bM(2x, t)$ term on the right hand side of the first equation in (1) arises due to a change of variable in the derivation as cells in an interval $[2x, 2x + 2\Delta x]$ are doubled in number and transferred to the interval $[x, x + \Delta x]$ with half the DNA content [12]. The term $I(x, t; T_S)$ denotes cells that have been T_S hours in DNA synthesis and are ready to be transferred to G_2 phase, which is also referred to as a delay term and its derivation is explained in [4]. However, $I(x, t; T_S)$ denotes the solution of the diffusion equation

$$\frac{\partial I(x, t; \tau_S)}{\partial \tau_S} + g \frac{\partial I(x, t; \tau_S)}{\partial x} - \varepsilon \frac{\partial^2 I(x, t; \tau_S)}{\partial x^2} + \mu_S I(x, t; \tau_S) = 0, \quad 0 < x < \infty, t > \tau_S > 0,$$

at time $\tau_S = T_S$, where τ_S is the time denoting the time spent by cells in DNA synthesis or S phase. The analytical solution (with appropriate initial conditions and a zero flux boundary condition) is obtained by using Laplace transform techniques and Green's functions in [12].

Thus, it reads

$$(2) \quad I(x, t, T_S) = \begin{cases} \int_0^\infty k_1 G_1(y, t - T_S) \gamma(T_S, x, y) dy, & \text{if } t \geq T_S, \\ I(x, t, T_S) = 0, & \text{if } t < T_S, \end{cases}$$

where $\gamma(T_S, x, y)$ denotes a weight function given by

$$(3) \quad \gamma(T_S, x, y) = \frac{\exp(-\mu_S \tau)}{2\sqrt{\pi \epsilon \tau}} \left(\exp\left(-\frac{((x - g\tau) - y)^2}{4\epsilon \tau}\right) - (1 + v(\tau, x, y)) \exp\left(-\frac{((x + g\tau) + y)^2}{4\epsilon \tau}\right) \right),$$

with

$$v(\tau, x, y) = \frac{x + y}{g\tau} (1 + O(\tau^{-1})).$$

In equation (3) γ denotes a Greens function whereas, v term arises due to the zero flux boundary condition.

The system (1) is incomplete without initial and boundary conditions. These conditions, which are chosen according to experimental evidence [12], take the form of

$$(4) \quad \left. \begin{aligned} G_1(x, 0) &= \frac{a_0}{\sqrt{2\pi\theta_0^2}} \exp\left(-\frac{(x-1)^2}{2\pi\theta_0^2}\right), \quad 0 < x < \infty, \\ S(x, 0) &= 0, \quad G_2(x, 0) = 0, \quad M(x, 0) = 0, \quad 0 < x < \infty, \end{aligned} \right\}$$

and the boundary condition

$$(5) \quad \epsilon \frac{\partial S(0, t)}{\partial x} - gS(0, t) = 0, \quad t > 0.$$

The initial DNA content of cells in the G_1 phase is chosen as a Gaussian distribution with relative mean DNA content at $x = 1$ equal to a_0 , and variance θ_0^2 . This variance is chosen sufficiently small so that the extension of $G_1(x, 0)$ into the in-feasible region $x < 0$ is of no significance. In [12] a numerical methods are constructed to solve (1) supplemented by the initial conditions in equation (4) and the general boundary conditions of the form of

$$(6) \quad \left. \begin{aligned} \epsilon \frac{\partial S(0, t)}{\partial x} - gS(0, t) &= \alpha, \quad t > 0, \\ S(L, 0) &= \beta, \quad t > 0, \end{aligned} \right\}$$

with any real values α and β , where the parameter β was chosen according to the experimental data provided in [5].

We can see that the system in equation (1) is a semi-system of integro-delayed partial differential equation (IDPDE). Thus, in order to have a complete understanding of the population kinetics of the human tumor cells, it is very important to include the spatial effects of all the cells in each phase, rather only consider the spatial effects of one phase and ignore the other effects of the other three phases. Consequently, mathematical analysis of the extended model is also vital to justify the understanding of the population kinetics of human tumor cells, when one present the experimental results. Therefore, our first aim in this paper, is to extend the model in equation (1) to a system of convection-reaction-diffusion equations, investigate the qualitative features of the model with the spatial effects of all the phases and determine the location of the boundary layer. Since, flow cytometry is a technique where the DNA content of individual cells is measured and binned accordingly, then we can see that our results present clearly the phases which are perturbed and unperturbed by the therapy. Thus, perturbation by cancer therapy causes these peaks to change in relation to one another as it can be seen in all the figures presented.

It is a well known fact that explicit methods such as the explicit finite difference methods (EFDMS), solve differential equations with low computational cost, within very small stability regions, which in turn implies severe restrictions on meshes sizes, which are required in order to achieve the desired results. Therefore, implicit finite difference methods (IFDMS) are more favored to solve differential equations, because of their wider stability regions as compared to the EFDMS [9]. Thus, our second aim in this paper, is to solve the extended model. Thus, we develop an efficient numerical method for solving the extended model with respect to the qualitative features of the original model.

Thus, extending the IDPDE in equation (1), we have

$$(7) \quad \left. \begin{aligned} \frac{\partial G_1(x,t)}{\partial t} &= D_{G_1} \frac{\partial^2 G_1(x,t)}{\partial x^2} + 4bM(2x,t) - (k_1 + \mu_{G_1})G_1(x,t), \\ \frac{\partial S(x,t)}{\partial t} &= \epsilon \frac{\partial^2 S(x,t)}{\partial x^2} - g \frac{\partial S(x,t)}{\partial x} - \mu_S S(x,t) + k_1 G_1(x,t) - I(x,t; T_S), \\ \frac{\partial G_2(x,t)}{\partial t} &= D_{G_2} \frac{\partial^2 G_2(x,t)}{\partial x^2} + I(x,t; T_S) - (k_2 + \mu_{G_2})G_2(x,t), \\ \frac{\partial M(x,t)}{\partial t} &= D_M \frac{\partial^2 M(x,t)}{\partial x^2} + k_2 G_2(x,t) - bM(x,t) - \mu_M M(x,t), \end{aligned} \right\}$$

where, D_{G_1}, D_{G_2}, D_M denote the dispersion coefficient of G_1, G_2 and M cells in each phase, $0 < x < L$ and $t > 0$, subject to the initial data as given in equation (4) and the boundary conditions are

$$(8) \quad \left. \begin{aligned} \frac{\partial G_1}{\partial \nu}(0, t) &= \frac{\partial G_2}{\partial \nu}(0, t) = \frac{\partial M}{\partial \nu}(0, t) = \chi_1, \\ \frac{\partial G_1}{\partial \nu}(L, t) &= \frac{\partial G_2}{\partial \nu}(L, t) = \frac{\partial M}{\partial \nu}(L, t) = \chi_2, \\ \varepsilon \frac{\partial S(0, t)}{\partial x} - gS(0, t) &= \alpha, \quad t > 0, \\ S(L, 0) &= \beta, \quad t > 0, \end{aligned} \right\}$$

where, $\nu, \chi_k, (k = 1, 2)$ denote an outward normal vector, and positive constants, whereas the initial functions $(G_1)_0(x, t), S_0(x, t), (G_2)_0(x, t), M_0(x, t)$ are assumed to satisfy the compatibility conditions [26],

$$(9) \quad \left. \begin{aligned} \frac{\partial G_1}{\partial \nu}(0, 0) &= \frac{\partial G_2}{\partial \nu}(0, 0) = \frac{\partial M}{\partial \nu}(0, 0) = \chi_1, \\ \frac{\partial G_1}{\partial \nu}(L, 0) &= \frac{\partial G_2}{\partial \nu}(L, 0) = \frac{\partial M}{\partial \nu}(L, 0) = \chi_2, \\ \varepsilon \frac{\partial S(0, 0)}{\partial x} - gS(0, 0) &= \alpha, \quad t > 0, \\ S(L, 0) &= \beta, \\ \frac{\partial G_1(0, 0)}{\partial t} &= D_{G_1} \frac{\partial^2 G_1(0, 0)}{\partial x^2} + 4bM(0, 0) - (k_1 + \mu_{G_1})G_1(0, 0), \\ \frac{\partial S(0, 0)}{\partial t} &= \varepsilon \frac{\partial^2 S(0, 0)}{\partial x^2} - g \frac{\partial S(0, 0)}{\partial x} - \mu_S S(0, 0) + k_1 G_1(0, 0) - I(0, 0; 0), \\ \frac{\partial G_2(0, 0)}{\partial t} &= D_{G_2} \frac{\partial^2 G_2(0, 0)}{\partial x^2} + I(0, 0; 0) - (k_2 + \mu_{G_2})G_2(0, 0), \\ \frac{\partial M(0, 0)}{\partial t} &= D_M \frac{\partial^2 M(0, 0)}{\partial x^2} + k_2 G_2(0, 0) - bM(0, 0) - \mu_M M(0, 0), \end{aligned} \right\}$$

and

$$\begin{aligned}
 & \frac{\partial G_1}{\partial v}(L, 0) = \frac{\partial G_2}{\partial v}(L, 0) = \frac{\partial M}{\partial v}(L, 0) = \chi_1, \\
 & \frac{\partial G_1}{\partial v}(L, 0) = \frac{\partial G_2}{\partial v}(L, 0) = \frac{\partial M}{\partial v}(L, 0) = \chi_2, \\
 & \varepsilon \frac{\partial S(L, 0)}{\partial x} - gS(L, 0) = \alpha, \quad t > 0, \\
 & S(L, 0) = \beta, \\
 & \frac{\partial G_1(L, 0)}{\partial t} = D_{G_1} \frac{\partial^2 G_1(L, 0)}{\partial x^2} + 4bM(L, 0) - (k_1 + \mu_{G_1})G_1(L, 0), \\
 & \frac{\partial S(L, 0)}{\partial t} = \varepsilon \frac{\partial^2 S(L, 0)}{\partial x^2} - g \frac{\partial S(L, 0)}{\partial x} - \mu_S S(L, 0) + k_1 G_1(L, 0) - I(L, 0; 0), \\
 & \frac{\partial G_2(L, 0)}{\partial t} = D_{G_2} \frac{\partial^2 G_2(L, 0)}{\partial x^2} + I(L, 0; 0) - (k_2 + \mu_{G_2})G_2(L, 0), \\
 & \frac{\partial M(L, 0)}{\partial t} = D_M \frac{\partial^2 M(L, 0)}{\partial x^2} + k_2 G_2(L, 0) - bM(L, 0) - \mu_M M(L, 0).
 \end{aligned}
 \tag{10}$$

Under the assumptions in (9-10) the extended model in equation (7) with the initial and boundary conditions in (8) has a unique solution [3].

The rest of the paper is arranged as follow. In Section 2, we carry out mathematical analysis of the model, whereas in Section 3, we derive and analyse the numerical method. Section 4 deals with the implementation of our numerical method, presentation of our numerical results and we conclude the paper with Section 5.

2. MATHEMATICAL ANALYSIS OF THE MODEL

At the steady states the model in equation (7) becomes

$$\begin{aligned}
 & D_{G_1} \frac{\partial^2 G_1(x, t)}{\partial x^2} - (k_1 + \mu_{G_1})G_1(x, t) = -4bM(2x, t), \\
 & \varepsilon \frac{\partial^2 S(x, t)}{\partial x^2} - g \frac{\partial S(x, t)}{\partial x} - \mu_S S(x, t) = I(x, t; T_S) - k_1 G_1(x, t), \\
 & D_{G_2} \frac{\partial^2 G_2(x, t)}{\partial x^2} - (k_2 + \mu_{G_2})G_2(x, t) = I(x, t; T_S), \\
 & D_M \frac{\partial^2 M(x, t)}{\partial x^2} - (b + \mu_M)M(x, t) = -k_2 G_2(x, t).
 \end{aligned}
 \tag{11}$$

From the first, third and fourth equations in (11) we obtain the following solutions for the corresponding homogeneous part

$$\begin{aligned}
 G_1^*(x) &= c_{g11} + c_{g12} \exp\left(\frac{D_{G_1}}{k_1 + \mu_{G_1}}x\right), \\
 G_2^*(x) &= c_{g21} + c_{g22} \exp\left(\frac{D_{G_2}}{k_2 + \mu_{G_2}}x\right), \\
 M^*(x) &= c_{m1} + c_{m2} \exp\left(\frac{D_M}{b + \mu_M}x\right),
 \end{aligned}
 \tag{12}$$

where, $c_{g11}, c_{g12}, c_{g21}, c_{g22}, c_{m1}, c_{m2}$ are non-negative constants. However, for the DNA synthesis or Sphase steady state, we see that the null space is given by

$$S'' - \frac{g}{\varepsilon}S' - \frac{\mu_S}{\varepsilon}S = 0,
 \tag{13}$$

of which the auxiliary equation to the equation (13) is

$$r^2 - \frac{g}{\varepsilon}r - \frac{\mu_S}{\varepsilon} = 0,
 \tag{14}$$

which implies that the solution to the auxiliary equation in (14) is

$$r^- = \frac{1}{2} \left(\frac{g}{\varepsilon} - \sqrt{\left(\frac{g}{\varepsilon}\right)^2 + 4\frac{\mu_S}{\varepsilon}} \right), \text{ and } r^+ = \frac{1}{2} \left(\frac{g}{\varepsilon} + \sqrt{\left(\frac{g}{\varepsilon}\right)^2 + 4\frac{\mu_S}{\varepsilon}} \right),
 \tag{15}$$

which in turn, implies that the solution to the second order differential equation in (13) is

$$S^* = A \exp(r^-x) + B \exp(r^+x),
 \tag{16}$$

where, from the given general boundary conditions in (8), we find that

$$A + B = S_0, \text{ and } S'_0 = Ar^- + Br^+,
 \tag{17}$$

so that

$$\begin{aligned} \varepsilon S_0' + gS_0 &= \alpha, \\ S_0' + \frac{g}{\varepsilon} S_0 &= \frac{\alpha}{\varepsilon}, \\ (18) \quad Ar^- + Br^+ + \frac{g}{\varepsilon}(A+B) &= \frac{\alpha}{\varepsilon}, \\ A(r^- + \frac{g}{\varepsilon}) + B(r^+ + \frac{g}{\varepsilon}) &= \frac{\alpha}{\varepsilon}, \\ A &= \frac{\frac{\alpha}{\varepsilon} - B(r^+ + \frac{g}{\varepsilon})}{(r^- + \frac{g}{\varepsilon})}. \end{aligned}$$

At $x = L$, the DNA synthesis or Sphase is prescribed as

$$\begin{aligned} \beta &= A \exp(r^-L) + B \exp(r^+L), \\ \beta &= \frac{\frac{\alpha}{\varepsilon} - B(r^+ + \frac{g}{\varepsilon})}{(r^- + \frac{g}{\varepsilon})} \exp(r^-L) + B \exp(r^+L), \\ \beta(r^- + \frac{g}{\varepsilon}) &= \frac{\alpha}{\varepsilon} - B(r^+ + \frac{g}{\varepsilon}) \exp(r^-L) + B \exp(r^+L)(r^- + \frac{g}{\varepsilon}), \\ \beta(r^- + \frac{g}{\varepsilon}) - \frac{\alpha}{\varepsilon} &= \left(\exp(r^+L)(r^- + \frac{g}{\varepsilon}) - (r^+ + \frac{g}{\varepsilon}) \exp(r^-L) \right) B, \\ (19) \quad B &= \frac{\beta(r^- + \frac{g}{\varepsilon}) - \frac{\alpha}{\varepsilon}}{(\exp(r^+L)(r^- + \frac{g}{\varepsilon}) - (r^+ + \frac{g}{\varepsilon}) \exp(r^-L))}. \end{aligned}$$

Substituting the value of B in (19) into equation (19) we obtain

$$(20) \quad A = \frac{\frac{\alpha}{\varepsilon}}{(r^- + \frac{g}{\varepsilon})} - \frac{(\beta(r^- + \frac{g}{\varepsilon}) - \frac{\alpha}{\varepsilon})(r^+ + \frac{g}{\varepsilon})}{(\exp(r^+L)(r^- + \frac{g}{\varepsilon}) - (r^+ + \frac{g}{\varepsilon}) \exp(r^-L)) (r^- + \frac{g}{\varepsilon})}.$$

This implies that the solution of the DNA synthesis or Sphase steady state, through the equation in (16) is

$$(21) \quad S^*(x, \varepsilon, g) = \frac{\frac{\alpha}{\varepsilon}}{(r^- + \frac{g}{\varepsilon})} - \frac{(\beta(r^- + \frac{g}{\varepsilon}) - \frac{\alpha}{\varepsilon})(r^+ + \frac{g}{\varepsilon})}{(\exp(r^+L)(r^- + \frac{g}{\varepsilon}) - (r^+ + \frac{g}{\varepsilon})\exp(r^-L))(r^- + \frac{g}{\varepsilon})} \exp(r^-x) \\ + \frac{\beta(r^- + \frac{g}{\varepsilon}) - \frac{\alpha}{\varepsilon}}{(\exp(r^+L)(r^- + \frac{g}{\varepsilon}) - (r^+ + \frac{g}{\varepsilon})\exp(r^-L))} \exp(r^+x).$$

Combining the equation in (21) with the steady-state solutions in equation (12), we have the local stability point $\mathcal{E} = (G_1^*, S^*, G_2^*, M^*)$, where,

$$(22) \quad \left. \begin{aligned} G_1^*(x) &= c_{g11} + c_{g12} \exp\left(\frac{D_{G_1}}{k_1 + \mu_{G_1}}x\right), \\ S^*(x, \varepsilon, g) &= \frac{\frac{\alpha}{\varepsilon}}{(r^- + \frac{g}{\varepsilon})} - \frac{(\beta(r^- + \frac{g}{\varepsilon}) - \frac{\alpha}{\varepsilon})(r^+ + \frac{g}{\varepsilon})}{(\exp(r^+L)(r^- + \frac{g}{\varepsilon}) - (r^+ + \frac{g}{\varepsilon})\exp(r^-L))(r^- + \frac{g}{\varepsilon})} \exp(r^-x) \\ &\quad + \frac{\beta(r^- + \frac{g}{\varepsilon}) - \frac{\alpha}{\varepsilon}}{(\exp(r^+L)(r^- + \frac{g}{\varepsilon}) - (r^+ + \frac{g}{\varepsilon})\exp(r^-L))} \exp(r^+x), \\ G_2^*(x) &= c_{g21} + c_{g22} \exp\left(\frac{D_{G_2}}{k_2 + \mu_{G_2}}x\right), \\ M^*(x) &= c_{m1} + c_{m2} \exp\left(\frac{D_M}{b + \mu_M}x\right). \end{aligned} \right\}$$

The steady point \mathcal{E} , enables us to present the behavior of the density of cells in each phase. Moreover, the steady state for the DNA synthesis or Sphase enables us to locate the boundary layer which is a result of perturbation by cancer therapy [12]. Thus, since the singularly perturbation occurs only during the DNA synthesis or Sphase, then it suffices to locate the layer by considering the solution to the steady state of the DNA synthesis or Sphase in equation (21). Thus, following [24] and the references there in, we see that

$$(23) \quad \lim_{x \rightarrow 0} \lim_{\varepsilon \rightarrow 0} S^*(x, \varepsilon, g) = \lim_{\varepsilon \rightarrow 0} \lim_{x \rightarrow 0} S^*(x, \varepsilon, g) \text{ and } \lim_{x \rightarrow L} \lim_{\varepsilon \rightarrow 0} S^*(x, \varepsilon, g) \neq \lim_{\varepsilon \rightarrow 0} \lim_{x \rightarrow L} S^*(x, \varepsilon, g),$$

then, the layer is located on the right-end of the interval, near $x = L$. This implies that, we are now in the position of deriving our numerical method.

3. DERIVATION AND ANALYSIS OF THE NUMERICAL METHOD

In this section, we describe the derivation of the fitted operator finite difference numerical method (FOFDM) for solving the G_1 phase, G_2 phase and metosis or M phase in equation (7) and non-standard finite difference method (NSFDM) for solving the DNA synthesis or S phase in equation (7). We first determine an approximation to the derivatives of the functions $G_1(t, x)$, $G_2(x, t)$ and $M(t, x)$ with respect to the spatial variable x .

Let N_x be a positive integer. Discretize the interval $[0, L]$ through the points

$$x_0 = 0 < x_1 < x_2 < \cdots < x_{N_x} = L,$$

where the step-size $\Delta x = x_{j+1} - x_j = L/N_x$, $j = 0, 1, \dots, x_{N_x}$. Let $(\mathcal{G}_1)_j(t)$, $(\mathcal{G}_2)_j(t)$, $\mathcal{M}_j(t)$ denote the numerical approximations of $G_1(t, j)$, $G_2(t, j)$, $M(t, j)$, then we approximate the second order spatial derivative by

$$\begin{aligned} \frac{\partial G_1}{\partial x^2}(t, x_j) &\approx \frac{(\mathcal{G}_1)_{j+1} - 2(\mathcal{G}_1)_j + (\mathcal{G}_1)_{j-1}}{(\phi_{G_1})_j^2}, \quad \frac{\partial G_2}{\partial x^2}(t, x_j) \approx \frac{(\mathcal{G}_2)_{j+1} - 2(\mathcal{G}_2)_j + (\mathcal{G}_2)_{j-1}}{(\phi_{G_2})_j^2}, \\ \frac{\partial M}{\partial x^2}(t, x_j) &\approx \frac{\mathcal{M}_{j+1} - 2\mathcal{M}_j + \mathcal{M}_{j-1}}{\phi_j^2}, \end{aligned} \quad (24)$$

where,

$$\begin{aligned} (\phi_{G_1})_j &= \frac{(1 - \exp((\sigma_{G_1})_j \Delta x))}{(\sigma_{G_1})_j}, \quad (\phi_{G_2})_j = \frac{(1 - \exp((\sigma_{G_2})_j \Delta x))}{(\sigma_{G_2})_j}, \\ (\phi_M)_j &= \frac{(1 - \exp((\sigma_M)_j \Delta x))}{(\sigma_M)_j}, \end{aligned} \quad (25)$$

and

$$(\sigma_{G_1})_j = \sqrt{\frac{k_1 + \mu_{G_1}}{D_{G_1}}}, \quad (\sigma_{G_2})_j = \sqrt{\frac{k_2 + \mu_{G_2}}{D_{G_2}}}, \quad (\sigma_M)_j = \sqrt{\frac{\mu_M + b}{D_M}}.$$

We see that $\phi_{G_1} \rightarrow \Delta x$ as $\Delta x \rightarrow 0$, $\phi_{G_2} \rightarrow \Delta x$ as $\Delta x \rightarrow 0$ and $\phi_M \rightarrow \Delta x$ as $\Delta x \rightarrow 0$.

Let N_t be a positive integer and $\Delta T = T/N_t$ where $0 < t < T$. Discretizing the time interval $[0, T]$ through the points

$$0 = t_0 < t_1 < \cdots < t_{N_t} = T,$$

where,

$$t_{n+1} - t_n = \Delta t, \quad n = 0, 1, \dots, (t_{N_t} - 1).$$

We approximate the time derivative at t_n by

$$(26) \quad \begin{aligned} \frac{d(\mathcal{G}_1)_j(t_n)}{dt} &\approx \frac{(\mathcal{G}_1)_j^{n+1} - (\mathcal{G}_1)_j^n}{\Psi_{G_1}}, & \frac{d(\mathcal{G}_2)_j(t_n)}{dt} &\approx \frac{(\mathcal{G}_2)_j^{n+1} - (\mathcal{G}_2)_j^n}{\Psi_{G_2}}, \\ \frac{d\mathcal{M}_j(t_n)}{dt} &\approx \frac{\mathcal{M}_j^{n+1} - \mathcal{M}_j^n}{\Psi_M}, \end{aligned}$$

where,

$$\begin{aligned} \Psi_{G_1} &= (\exp((k_1 + \mu_{G_1})\Delta t) - 1)/(k_1 + \mu_{G_1}), & \Psi_{G_2} &= (\exp((k_2 + \mu_{G_2})\Delta t) - 1)/(k_2 + \mu_{G_2}), \\ \Psi_M &= (\exp((b + \mu_M)\Delta t) - 1)/(b + \mu_M), \end{aligned}$$

where we see that $\Psi_{G_1} \rightarrow \Delta t$ as $\Delta t \rightarrow 0$, $\Psi_{G_2} \rightarrow \Delta t$ as $\Delta t \rightarrow 0$ and $\Psi_M \rightarrow \Delta t$ as $\Delta t \rightarrow 0$.

Next we develop the numerical method to solve the DNA synthesis or Sphase in equation (7). Since the FOFDM and SFDM fail to capture the hyperbolic nature of the advection-diffusion-reaction PDEs, below we follow the development in [16] to derive the NSFDM for the equation modeling the DNA synthesis or Sphase in equation (7). We proceed as follow. Let $\mathcal{S}_j(t)$ denote the numerical approximations of $S(t, j)$, then using the following sub-equations of the equation modeling the DNA synthesis or Sphase in equation (7)

$$(27) \quad \left. \begin{aligned} \frac{\partial S(x,t)}{\partial t} + g \frac{\partial S(x,t)}{\partial x} &= -\mu_S S(x,t), \text{ a PDE,} \\ g \frac{\partial S(x,t)}{\partial x} &= \varepsilon \frac{\partial^2 S(x,t)}{\partial x^2}, \text{ an ODE,} \end{aligned} \right\}$$

then the exact finite difference schemes for the two sub-equations in equation (27) are

$$(28) \quad \left. \begin{aligned} \frac{\mathcal{S}_j^{n+1} - \mathcal{S}_j^n}{(\phi_1)_S(\Delta t)} + g \frac{\mathcal{S}_{j+1}^{n+1} - \mathcal{S}_j^{n+1}}{g(\phi_1)_S(\frac{\Delta x}{g})} &= -\mu_S \mathcal{S}_j^n, \text{ a scheme for a PDE} \\ \frac{\mathcal{S}_{j+1} - \mathcal{S}_j}{\Delta x} &= \varepsilon \frac{\mathcal{S}_{j+1} - 2\mathcal{S}_j + \mathcal{S}_{j-1}}{\frac{\varepsilon \Delta x}{g}(\phi_2)_S(\Delta x)}, \text{ a scheme for an ODE,} \end{aligned} \right\}$$

where $(\phi_1)_S(\Delta t) = (1 - \exp(-\mu_S \Delta t))/\mu_S$ and $(\phi_2)_S(\Delta x) = (1 - \exp(-\frac{g \Delta x}{\varepsilon}))$. Combining the exact finite difference schemes in equation (28) and avoid the condition $g \Delta t = \Delta x$, we obtain

the NSFDM for the DNA phase as

$$(29) \quad \frac{\mathcal{S}_j^{n+1} - \mathcal{S}_j^n}{(\phi_1)_S(\Delta t)} + g \frac{\mathcal{S}_{j+1}^{n+1} - \mathcal{S}_j^{n+1}}{g(\phi_1)_S(\frac{\Delta x}{g})} = \varepsilon \frac{\mathcal{S}_{j+1}^{n+1} - 2\mathcal{S}_j^{n+1} + \mathcal{S}_{j-1}^{n+1}}{\varphi(\Delta x)} - \mu_S \mathcal{S}_j^n + k_1(\mathcal{G}_1)_j^n - I(x, t; T_S).$$

where $\varphi(\Delta x) = g\phi_S(\frac{\Delta x}{g})\frac{\varepsilon\Delta x}{g}(\phi_2)_S(\Delta x)$. We see that $\phi_S \rightarrow \Delta x$ as $\Delta x \rightarrow 0$. Similarly for $\varphi(\Delta x)$. The denominator functions in equations (24), (26) and (28) are used explicitly to remove the inherent stiffness in the central finite derivatives parts and can be derived by using the theory of nonstandard finite difference methods, see, e.g., [15, 22, 23] and references therein.

Combining the equation (24) for the spatial derivatives with the equation (26) for time derivatives and with equation in (29), we obtain the system of FOFDM-NSFDM as

$$(30) \quad \left. \begin{aligned} \frac{(\mathcal{G}_1)_j^{n+1} - (\mathcal{G}_1)_j^n}{\phi_{G_1}} &= D_{G_1} \frac{(\mathcal{G}_1)_{j+1}^{n+1} - 2(\mathcal{G}_1)_j^{n+1} + (\mathcal{G}_1)_{j-1}^{n+1}}{(\phi_{G_1})_j^2} + 4b\mathcal{M}_{2j}^n - (k_1 + \mu_{G_1})(\mathcal{G}_1)_j^n, \\ \frac{\mathcal{S}_j^{n+1} - \mathcal{S}_j^n}{(\phi_1)_S(\Delta t)} + g \frac{\mathcal{S}_{j+1}^{n+1} - \mathcal{S}_j^{n+1}}{g(\phi_1)_S(\frac{\Delta x}{g})} &= \varepsilon \frac{\mathcal{S}_{j+1}^{n+1} - 2\mathcal{S}_j^{n+1} + \mathcal{S}_{j-1}^{n+1}}{\varphi(\Delta x)} - \mu_S \mathcal{S}_j^n + k_1(\mathcal{G}_1)_j^n - I(x, t; T_S), \\ \frac{(\mathcal{G}_2)_j^{n+1} - (\mathcal{G}_2)_j^n}{\phi_{G_2}} &= D_{G_2} \frac{(\mathcal{G}_2)_{j+1}^{n+1} - 2(\mathcal{G}_2)_j^{n+1} + (\mathcal{G}_2)_{j-1}^{n+1}}{(\phi_{G_2})_j^2} + I(x, t; T_S) - (k_2 + \mu_{G_2})(\mathcal{G}_2)_j^n, \\ \frac{\mathcal{M}_j^{n+1} - \mathcal{M}_j^n}{\phi_M} &= D_M \frac{\mathcal{M}_{j+1}^{n+1} - 2\mathcal{M}_j^{n+1} + \mathcal{M}_{j-1}^{n+1}}{(\phi_M)_j^2} + k_2(\mathcal{G}_2)_j^n - (b + \mu_M)\mathcal{M}_j^n, \\ (\mathcal{G}_1)_1^n &= (\mathcal{G}_1)_{-1}^n, (\mathcal{G}_2)_1^n = (\mathcal{G}_2)_{-1}^n, \mathcal{S}_1^n = \mathcal{S}_{-1}^n, \mathcal{M}_1^n = \mathcal{M}_{-1}^n \\ (\mathcal{G}_1)_{x_{N_x}}^n &= (\mathcal{G}_1)_{x_{N_x}-1}^n, (\mathcal{G}_2)_{x_{N_x}}^n = (\mathcal{G}_2)_{x_{N_x}-1}^n, \mathcal{S}_{x_{N_x}}^n = \mathcal{S}_{x_{N_x}-1}^n, \mathcal{M}_{x_{N_x}}^n = \mathcal{M}_{x_{N_x}-1}^n, \\ (\mathcal{G}_1)_j^0 &= \frac{a_0}{\sqrt{2\pi\theta_0^2}} \exp\left(-\frac{(x_j-1)^2}{2\pi\theta_0^2}\right), (\mathcal{G}_2)_j^0 = 0, \mathcal{S}_j^0 = 0, \mathcal{M}_j^0 = 0. \end{aligned} \right\}$$

The system in equation (30) can further be simplified as

$$(31) \quad \left. \begin{aligned} -\frac{D_{G_1}}{(\phi_{G_1})_j^2} (\mathcal{G}_1)_{j-1}^{n+1} + \left(\frac{1}{\phi_{G_1}} + \frac{2D_{G_1}}{(\phi_{G_1})_j^2}\right) (\mathcal{G}_1)_j^{n+1} - \frac{D_{G_1}}{(\phi_{G_1})_j^2} (\mathcal{G}_1)_{j+1}^{n+1} \\ &= \left(\frac{1}{\phi_{G_1}} - (k_1 + \mu_{G_1})\right) (\mathcal{G}_1)_j^n + 4b\mathcal{M}_{2j}^n, \\ -\frac{\varepsilon}{\varphi(\Delta x)} \mathcal{S}_{j-1}^{n+1} + \left(\frac{1}{(\phi_1)_S(\Delta t)} - \frac{g}{(\phi_1)_S(\frac{\Delta x}{g})} + \frac{2\varepsilon}{\varphi(\Delta x)}\right) \mathcal{S}_j^{n+1} + \left(\frac{g}{(\phi_1)_S(\frac{\Delta x}{g})} - \frac{\varepsilon}{\varphi(\Delta x)}\right) \mathcal{S}_{j+1}^{n+1} \\ &= \left(\frac{1}{(\phi_1)_S(\Delta t)} - \mu_S\right) \mathcal{S}_j^n + k_1(\mathcal{G}_1)_j^n - I(x, t; T_S), \\ -\frac{D_{G_2}}{(\phi_{G_2})_j^2} (\mathcal{G}_2)_{j-1}^{n+1} + \left(\frac{1}{\phi_{G_2}} + \frac{D_{G_2}}{(\phi_{G_2})_j^2}\right) (\mathcal{G}_2)_j^{n+1} - \frac{D_{G_2}}{(\phi_{G_2})_j^2} (\mathcal{G}_2)_{j+1}^{n+1} \\ &= \left(\frac{1}{\phi_{G_2}} - (k_2 + \mu_{G_2})\right) (\mathcal{G}_2)_j^n + I(x, t; T_S), \\ -\frac{D_M}{(\phi_M)_j^2} \mathcal{M}_{j-1}^{n+1} + \left(\frac{1}{\phi_M} + \frac{D_M}{(\phi_M)_j^2}\right) \mathcal{M}_j^{n+1} - \frac{D_M}{(\phi_M)_j^2} \mathcal{M}_{j+1}^{n+1} \\ &= \left(\frac{1}{\phi_M} - (b + \mu_M)\right) \mathcal{M}_j^n + k_2(\mathcal{G}_2)_j^n. \end{aligned} \right\}$$

The system in equation (31) can be written as a tridiagonal system given by

$$(32) \quad \left. \begin{aligned} \mathcal{A}_{G_1}(\mathcal{G}_1) &= \mathcal{F}_{G_1}, \\ \mathcal{A}_S \mathcal{S} &= \mathcal{F}_S, \\ \mathcal{A}_{G_2}(\mathcal{G}_2) &= \mathcal{F}_{G_2}, \\ \mathcal{A}_M \mathcal{M} &= \mathcal{F}_M, \end{aligned} \right\}$$

where, $j = 1, \dots, x_{N_x} - 1$, $n = 0, \dots, t_{N_t} - 1$ and

$$\left. \begin{aligned} \mathcal{A}_{G_1} &= \text{Tri} \left(-\frac{D_{G_1}}{(\phi_{G_1})_j^2}, \frac{1}{\phi_{G_1}} + \frac{2D_{G_1}}{(\phi_T)_j^2}, -\frac{D_{G_1}}{(\phi_{G_1})_j^2} \right), \\ \mathcal{A}_S &= \text{Tri} \left(-\frac{\varepsilon}{\phi(\Delta x)}, \frac{1}{(\phi_1)_S(\Delta t)} - \frac{g}{(\phi_1)_S(\frac{\Delta x}{g})} + \frac{2\varepsilon}{\phi(\Delta x)}, -\frac{\varepsilon}{\phi(\Delta x)} \right), \\ \mathcal{A}_{G_2} &= \text{Tri} \left(-\frac{D_{G_2}}{(\phi_{G_2})_j^2}, \frac{1}{\phi_{G_2}} + \frac{D_{G_2}}{(\phi_{G_2})_j^2}, -\frac{D_{G_2}}{(\phi_{G_2})_j^2} \right), \\ \mathcal{A}_M &= \text{Tri} \left(-\frac{D_M}{(\phi_M)_j^2}, \frac{1}{\phi_M} + \frac{D_M}{(\phi_M)_j^2}, -\frac{D_M}{(\phi_M)_j^2} \right), \end{aligned} \right\}$$

and

$$\left. \begin{aligned} (\mathcal{F}_{G_1})_j^n &= \left(\frac{1}{\phi_{G_1}} - (k_1 + \mu_{G_1}) \right) (\mathcal{G}_1)_j^n + 4b \mathcal{M}_{2j}^n, \\ (\mathcal{F}_S)_j^n &= \left(\frac{1}{\phi_S(k)} - \mu_S \right) \mathcal{S}_j^n + k_1 (\mathcal{G}_1)_j^n - I(x, t; T_S), \\ (\mathcal{F}_{G_2})_j^n &= \left(\frac{1}{\phi_{G_2}} - (k_2 + \mu_{G_2}) \right) (\mathcal{G}_2)_j^n + I(x, t; T_S), \\ (\mathcal{F}_M)_j^n &= \left(\frac{1}{\phi_M} - (b + \mu_M) \right) \mathcal{M}_j^n + k_2 (\mathcal{G}_2)_j^n. \end{aligned} \right\}$$

Thus, in view of equation (32), we see that the local truncation errors $((\zeta_{G_1})_j^n, (\zeta_S)_j^n, (\zeta_{G_2})_j^n, (\zeta_M)_j^n)$ are given by

$$(33) \quad \left. \begin{aligned} (\zeta_{G_1})_j^n &= (\mathcal{A}_{G_1} G_1)_j^n - (F_{G_1})_j^n = (\mathcal{A}_{G_1} (G_1 - \mathcal{G}_1))_j^n, \\ (\zeta_S)_j^n &= (\mathcal{A}_S S)_j^n - (F_S)_j^n = (\mathcal{A}_S (S - \mathcal{S}))_j^n, \\ (\zeta_{G_2})_j^n &= (\mathcal{A}_{G_2} \mathcal{G}_2)_j^n - (F_{G_2})_j^n = (\mathcal{A}_{G_2} (G_2 - \mathcal{G}_2))_j^n, \\ (\zeta_M)_j^n &= (\mathcal{A}_M \mathcal{M})_j^n - (F_M)_j^n = (\mathcal{A}_M (M - \mathcal{M}))_j^n. \end{aligned} \right\}$$

Thus,

$$(34) \quad \left. \begin{aligned} \max_{1 \leq n \leq T, 1 \leq j \leq L} |(G_1)_j^n - (\mathcal{G}_1)_j^n| &\leq \|(\mathcal{A}_{G_1})^{-1}\| |(\zeta_{G_1})_j^n|, \\ \max_{1 \leq n \leq T, 1 \leq j \leq L} |S_j^n - \mathcal{S}_j^n| &\leq \|(\mathcal{A}_S)^{-1}\| |(\zeta_S)_j^n|, \\ \max_{1 \leq n \leq T, 1 \leq j \leq L} |(G_2)_j^n - (\mathcal{G}_2)_j^n| &\leq \|(\mathcal{A}_{G_2})^{-1}\| |(\zeta_{G_2})_j^n|, \\ \max_{1 \leq n \leq T, 1 \leq j \leq L} |M_j^n - \mathcal{M}_j^n| &\leq \|(\mathcal{A}_M)^{-1}\| |(\zeta_M)_j^n|, \end{aligned} \right\}$$

where

$$(35) \quad \left. \begin{aligned} \max_{1 \leq n-1 \leq T, 1 \leq j \leq L-1} |(\zeta_{G_1})_j^n| &\leq \frac{\Delta t}{2} |(G_1)_{tt}(\zeta)| + D_{G_1} \frac{(\Delta x)^2}{12} |(G_1)_{xxxx}(\xi)|, \\ \max_{1 \leq n-1 \leq T, 1 \leq j \leq L-1} |(\zeta_S)_j^n| &\leq \frac{\Delta t}{2} |S_{tt}(\zeta)| + g \frac{\Delta x}{2} |S_{xx}(\xi)| + \varepsilon \frac{(\Delta x)^2}{12} |S_{xxxx}(\xi)|, \\ \max_{1 \leq n-1 \leq T, 1 \leq j \leq L-1} |(\zeta_{G_2})_j^n| &\leq \frac{\Delta t}{2} |(G_2)_{tt}(\zeta)| + D_{G_2} \frac{(\Delta x)^2}{12} |(G_2)_{xxxx}(\xi)|, \\ \max_{1 \leq n-1 \leq T, 1 \leq j \leq L-1} |(\zeta_M)_j^n| &\leq \frac{\Delta t}{2} |M_{tt}(\zeta)| - D_M \frac{(\Delta x)^2}{12} |M_{xxxx}(\xi)|, \end{aligned} \right\}$$

where $t_{n-1} \leq \zeta \leq t_{n+1}$, $x_{j-1} \leq \xi \leq x_{j+1}$ and by [27] we have

$$(36) \quad \|(\mathcal{A}_{G_1})^{-1}\| \leq \Xi_{G_1}, \|(\mathcal{A}_S)^{-1}\| \leq \Xi_S, \|(\mathcal{A}_{G_2})^{-1}\| \leq \Xi_{G_2}, \|(\mathcal{A}_M)^{-1}\| \leq \Xi_M.$$

Using (35) and (36) in (34), we obtain

$$(37) \quad \left. \begin{aligned} \max_{1 \leq n \leq T, 1 \leq j \leq L} |(G_1)_j^n - (\mathcal{G}_1)_j^n| &\leq |\Xi_{G_1}| \left[\frac{\Delta t}{2} |(G_1)_{tt}(\zeta)| + D_{G_1} \frac{(\Delta x)^2}{12} |(G_1)_{xxxx}(\xi)| \right], \\ \max_{1 \leq n \leq T, 1 \leq j \leq L} |S_j^n - \mathcal{S}_j^n| &\leq |\Xi_S| \left[\frac{\Delta t}{2} |S_{tt}(\zeta)| + g \frac{\Delta x}{2} |S_{xx}(\xi)| + \varepsilon \frac{(\Delta x)^2}{12} |S_{xxxx}(\xi)| \right], \\ \max_{1 \leq n \leq T, 1 \leq j \leq L} |(G_2)_j^n - (\mathcal{G}_2)_j^n| &\leq |\Xi_{G_2}| \left[\frac{\Delta t}{2} |(G_2)_{tt}(\zeta)| + D_{G_2} \frac{(\Delta x)^2}{12} |(G_2)_{xxxx}(\xi)| \right], \\ \max_{1 \leq n \leq T, 1 \leq j \leq L} |M_j^n - \mathcal{M}_j^n| &\leq |\Xi_M| \left[\frac{\Delta t}{2} |M_{tt}(\zeta)| - D_M \frac{(\Delta x)^2}{12} |M_{xxxx}(\xi)| \right]. \end{aligned} \right\}$$

Hence, we obtain the following results.

Theorem 3.1. Let $F_{G_1}(x, t), F_S(x, t), F_{G_2}(x, t), F_M(x, t)$ be sufficiently smooth functions so that $G_1(x, t), S(x, t), G_2(x, t), M(x, t) \in C^{1,2}([1, L] \times [1, T])$. Let $(\mathcal{G}_1)_j^n, \mathcal{S}_j^n, (\mathcal{G}_2)_j^n, \mathcal{M}_j^n, j = 1, 2, \dots, L, n = 1, 2, \dots, T$ be the approximate solutions to (7), obtained using the FOFDM-NSFDM with $(\mathcal{G}_1)_j^0 = (G_1)_j^0, \mathcal{S}_j^0 = S_j^0, (\mathcal{G}_2)_j^0 = (G_2)_j^0, \mathcal{M}_j^0 = M_j^0$. Then there exists $\Xi_{G_1}, \Xi_S, \Xi_{G_2}, \Xi_M$ independent of g, ε , the step sizes Δt and Δx such that

$$\left. \begin{aligned} \sup_{0 < \varepsilon \leq 1, g > > 1} \max_{1 \leq n \leq T, 1 \leq j \leq L} |(G_1)_j^n - (\mathcal{G}_1)_j^n| &\leq |\Xi_{G_1}| \left[\frac{\Delta t}{2} |(G_1)_{tt}(\zeta)| + D_{G_1} \frac{(\Delta x)^2}{12} |(G_1)_{xxxx}(\xi)| \right], \\ \sup_{0 < \varepsilon \leq 1, g > > 1} \max_{1 \leq n \leq T, 1 \leq j \leq L} |S_j^n - \mathcal{S}_j^n| &\leq |\Xi_S| \left[\frac{\Delta t}{2} |S_{tt}(\zeta)| + g \frac{\Delta x}{2} |S_{xx}(\xi)| + \varepsilon \frac{(\Delta x)^2}{12} |S_{xxxx}(\xi)| \right], \\ \sup_{0 < \varepsilon \leq 1, g > > 1} \max_{1 \leq n \leq T, 1 \leq j \leq L} |(G_2)_j^n - (\mathcal{G}_2)_j^n| &\leq |\Xi_{G_2}| \left[\frac{\Delta t}{2} |(G_2)_{tt}(\zeta)| + D_{G_2} \frac{(\Delta x)^2}{12} |(G_2)_{xxxx}(\xi)| \right], \\ \sup_{0 < \varepsilon \leq 1, g > > 1} \max_{1 \leq n \leq T, 1 \leq j \leq L} |M_j^n - \mathcal{M}_j^n| &\leq |\Xi_M| \left[\frac{\Delta t}{2} |M_{tt}(\zeta)| - D_M \frac{(\Delta x)^2}{12} |M_{xxxx}(\xi)| \right]. \end{aligned} \right\}$$

This shows that our FOFDM-NSFDM are unconditionally stable.

4. NUMERICAL RESULTS AND DISCUSSIONS

Setting $D_{G_1} = 10^{-4}, D_{G_2} = 10^{-4}, D_M = 10^{-7}, L = 5, T = 1, x_{N_x} = t_{N_t} = 20$ and , we present our numerical solutions in Figure 1 (for $\varepsilon = 0.001$), Figure 2 (for $\varepsilon = 0.01$), Figure 3 (for $\varepsilon = 0.1$) using the parameter values [4] in Table 1.

TABLE 1. Parameter values [4]

$k_1 = 0.8$	$\mu_{G_1} = 0.9$	$\alpha = 2.4$	$g = 30.9$
$\theta_0 = 0.6$	$\mu_S = 0.8$	$\beta = 0.1$	$k_2 = 0.0193$
$\mu_{G_2} = 2$	$b = 1.9296$	$\mu_M = 0.01$	$a_0 = 100.0$

In Figure 1(a), we see that as time grows the density of cells are increasing within the range of approximately of $x \in (0, 1.5)$, then for the values of $x \in (1.5, 5)$, the profile presents that there are no more cells available for G_1 phase.

In Figure 1(b), we see that as time grows the density of cells form a peak which is increasing within the range of approximately of the values of $x \in (0, 1.5)$, then for the values of $x \in (1.5, 5)$ the density of cells converges to its low positive steady state.

In Figure 1(c), we see the contrary to the profiles of the two previous profiles. That, as time grows the density of cells grows exponentially for $x \in (0, 1.5)$, till they reach a positive steady state for $x \in (1.5, 5)$. The profile of this phase presents that all cells are well and active for next interactions.

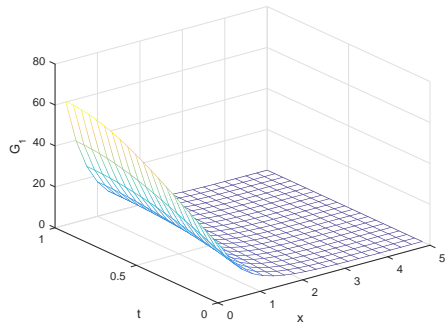
In Figure 1(d), we see similar development compare to the interactions in the M phase, that as time grows the density of cells grows exponentially for the values of $x \in (0, 1.5)$, till they reach a positive steady state for $x \in (1.5, 5)$. The profile of this phase presents that all cells are well and active for the next interaction.

The remaining two figures, Figure 2 and Figure 3, we have the same profiles as in Figure 1, for different values of $\varepsilon \in (0, 1)$.

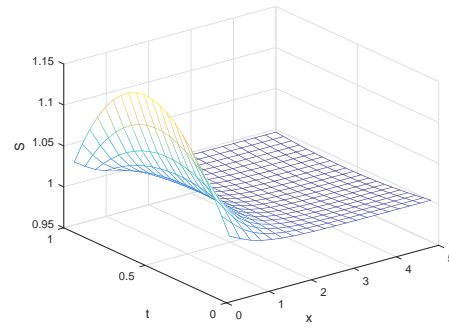
5. CONCLUSION

In this paper, we extended the model for population kinetics of human tumor in vitro, with the aim to contribute toward the understanding of cells cycle in each phase. This is very essential toward healing cancer as a dreadful disease, since in [12] categorically mentioned that even in the simplified environment of the laboratory with modern technology it is not always possible to isolate the effects of cancer treatment on the cell cycle of human cancer lines. Thus, in view of our numerical results, we see that for the values of $0 < \varepsilon \lll 1$ and $g \ggg 1$ our numerical

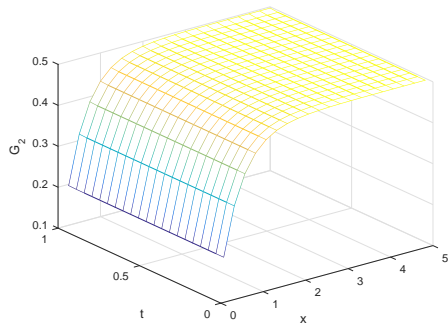
solutions are the same, despite the fact that cells population behave differently in each phase. As time goes, we see that during G_1 phase, that the cells grow sharply to a very high height as time increases, but for certain different positions only. During the DNA synthesis or S phase, we see different peaks for certain different positions only as time increases, unlike for the G_2 phase and the metosis M phase, where we see that the cells grow sharply to their respective uniform steady states. These growths are due to the steady states presented in (22). When we decrease the value for the division rate parameter (b), then the behavior of the metosis or M phase changes to a linear growth rate, whereas increasing the division rate (b), changes the growth rate a parabolic growth rate (results not shown). Other changes in the parameter values does not bring new phenomena, except for the fact that $\mu_S \neq 0$, because we believe a small amount cells should at least be exiting the phase, during this phase too. We also see an important feature in our numerical results that notable interactions takes place at certain positions only in all the phases. This, we believe can contribute quite a great deal toward understanding of cells cycle in each phase, which in turn can be taken up for further cancer research on the cell cycle of human cancer lines. Thus, our approach in this work should serve as a first attempt to incorporate the detailed effects of population kinetics of human tumor. Hence, our future direction is to carry out comparison with the latest reported method(s) in the subsequent recent years' papers.



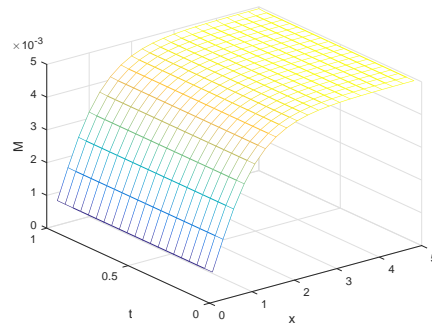
(a) Behaviour of G_1 phase



(b) Behaviour of DNA synthesis or S phase

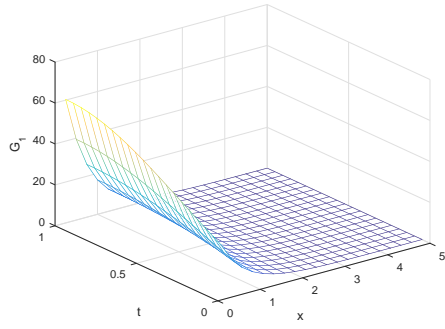
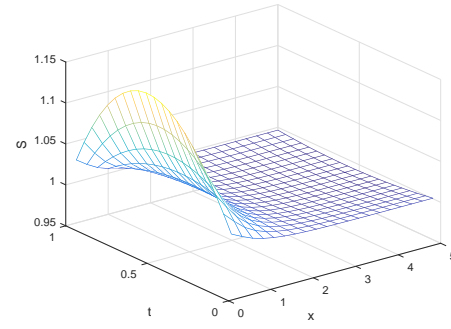
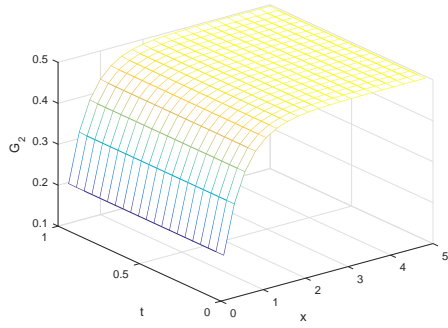
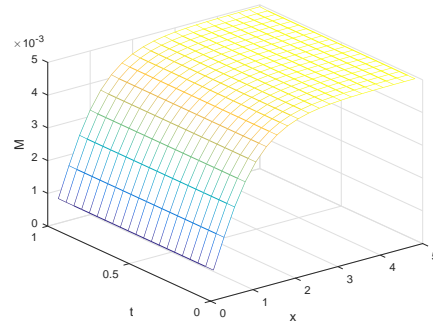


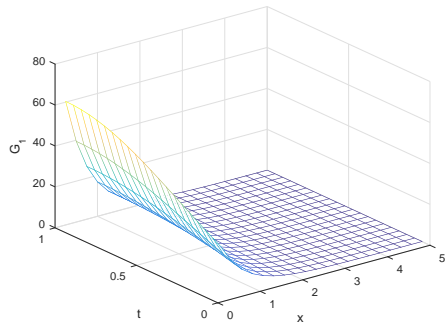
(c) Behaviour of G_2 phase



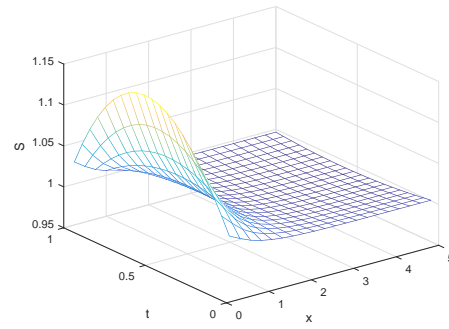
(d) Behaviour of metosis or M phase

FIGURE 1. FOFDM-NSFDM numerical solution of the system in (30) for $\varepsilon = 0.001$.

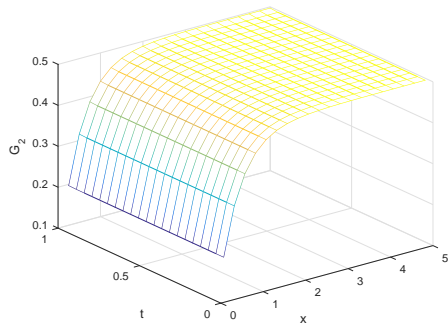
(a) Behaviour of G_1 phase(b) Behaviour of DNA synthesis or S phase(c) Behaviour of G_2 phase(d) Behaviour of metosis or M phaseFIGURE 2. FOFDM-NSFDM numerical solution of the system in (30) for $\varepsilon = 0.01$.



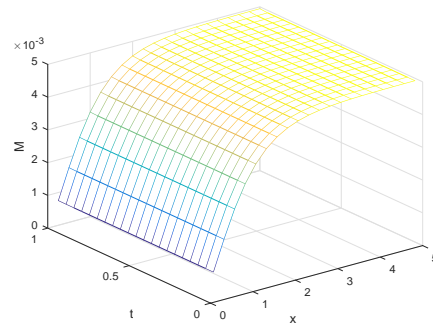
(a) Behaviour of G_1 phase



(b) Behaviour of DNA synthesis or S phase



(c) Behaviour of G_2 phase



(d) Behaviour of metosis or M phase

FIGURE 3. FOFDM-NSFDM numerical solution of the system in (30) for $\varepsilon = 0.1$.

ACKNOWLEDGMENTS

We would like to thank the University of the Western Cape for the NRF support.

CONFLICT OF INTERESTS

The author(s) declare that there is no conflict of interests.

REFERENCES

- [1] B. Alberts, A. Johnson, J. Lewis, M. Raff, K. Roberts and P. Walter, *Molecular Biology of the Cell*, New York, 2002.
- [2] C.N. Amaya, D.C. Mitchell and B.A. Bryan, Rho kinase proteins display aberrant up regulation in vascular tumors and contribute to vascular tumor growth, *BMC Cancer*, 17 (2017), 485.
- [3] A.R. Ansari, S.A. Bakr and G.I. Shishkin, A parameter-robust finite difference method for singularly perturbed parabolic partial differential equations, *J. Comput. Appl. Math.* 205 (2007), 552-566.
- [4] B. Basse, B.C. Baguley, E.S. Marshall and W.R. Joseph, A mathematical model for analysis of the cell cycle in cell lines derived from human tumours, *J. Math. Biol.* 47 (2003), 295-312.
- [5] B. Basse, B.C. Baguley, E.S. Marshall, G.C. Wake and D.J.N. Wall, Modelling cell population growth with applications to cancer therapy in human tumor cell lines, *Prog. Biophys. Mol. Biol.* 85 (2004), 353-368.
- [6] B. Basse, B.C. Baguley, E.S. Marshall, G.C. Wake and D.J.N. Wall, Modelling the flow cytometric data obtained from unperturbed human tumour cell lines: Parameter fitting and comparison, *Bull. Math. Biol.* 67 (2005), 815-830.
- [7] B. Basse and P. Ubezio, A generalised age and phase structured model of human tumour cell populations both unperturbed and exposed to a range of cancer therapies, *Bull. Math. Biol.* 69(5) (2007), 1673-1690.
- [8] B. Basse, G.C. Wake, D.J.N. Wall and B. van Brunt, On a cell growth model for plankton, *Math. Med. Biol.* 21 (2004), 49-61.
- [9] J.C. Butcher, Implicit Runge-Kutta processes, *Math. Comput.* 18(85) (1964), 50-64.
- [10] R. D'Ambrosio and B. Paternoster, Numerical solution of a diffusion problem by exponentially fitted finite difference methods, *SpringerPlus* 3(1) (2014), 425.
- [11] B. Giotti, A. Joshi, and T.C. Freeman, Meta-analysis reveals conserved cell cycle transcriptional network across multiple human cell types, *BMC Genomics* 18 (2017), 30.
- [12] Z. Jackiewicz, B. Zubik-Kowal and B. Basse, Finite-difference and Pseudo-spectral methods for the numerical Simulations of in vitro human tumour cell population kinetics, *Math. Biosci. Eng.* 6(3) (2009), 561-572.

- [13] D. Kulkarni, D. Schmidt and S.K. Tsui, Eigenvalues of tridiagonal pseudo-Toeplitz matrices, *Linear Algebra Appl.* 297 (1999), 63-80.
- [14] F. Maldaran and J. Izadian, Two numerical methods for simulation of in vitro human tumour cell population kinetics, *Acta Comput.* 1 (2012) 149-153.
- [15] R.E. Mickens, *Nonstandard Finite Difference Models of Differential Equations*, World Scientific, Singapore, 1994.
- [16] R.E. Mickens (editor), *Applications of Nonstandard Finite Difference Schemes*, World Scientific, Singapore, 2000.
- [17] S. Noschese, L. Pasquini and L. Reichel, Tridiagonal Toeplitz matrices: Properties and novel applications, *Numer. Linear Algebra Appl.* 20(2) (2013), 302-326.
- [18] K.M. Owolabi, K.C. Patidar and A. Shikongo, Mathematical analysis and numerical simulation of a tumor-host model with chemotherapy application, *Commun. Math. Biol. Neurosci.* 2018 (2018), 21.
- [19] K.M. Owolabi, K.C. Patidar and A. Shikongo, Efficient numerical method for a model arising in biological stoichiometry of tumour dynamics, *Discrete Contin. Dyn. Syst., Ser. S* 12(3) (2019), 591-613.
- [20] K.M. Owolabi, K.C. Patidar and A. Shikongo, A fitted numerical method for a model arising in HIV related cancer-immune system dynamics, *Commun. Math. Biol. Neurosci.* 2019 (2019), 1.
- [21] K.M. Owolabi, K.C. Patidar and A. Shikongo, Numerical solution for a problem arising in angiogenic signaling, *AIMS Math.* 4(1) (2019) 43-63.
- [22] K.C. Patidar, On the use of non-standard finite difference methods, *J. Difference Equ. Appl.* 11 (2005), 735-758.
- [23] K.C. Patidar, Nonstandard finite difference methods: recent trends and further developments, *J. Difference Equ. Appl.* 22(6) (2016), 817-849.
- [24] K.C. Patidar and A. Shikongo, The Application of Asymptotic Analysis for Developing Reliable Numerical Method for a Model Singular Perturbation Problem, *J. Numer. Anal. Ind. Appl. Math.* 2(3-4) (2007), 193-207.
- [25] C. Pavo, *Nonlinear parabolic and elliptic equations*, Library of Congress Cataloging in Publication Data, New York and London, 1992.
- [26] M.H. Protter and H.F. Weinberger, *Maximum Principles in Differential Equations*, Prentice Hall, Englewood Cliffs, New York, 1967.
- [27] P.N. Shivakumar and K. Ji, Upper and lower bounds for inverse elements of finite and infinite tridiagonal matrices, *Linear Algebra Appl.* 247 (1996), 297-316.
- [28] L. Spinelli, A. Torricelli, P. Ubezio and B. Basse, Modelling the balance between quiescence and cell death in normal and tumour cell populations, *Math. Biosci.* 202 (2006), 349-370.

- [29] J.M. Varah, A lower bound for the smallest singular value of a matrix, *Linear Algebra Appl.* 11 (1975), 3-5.
- [30] J.G. Verwer and J.M. Sanz-Serna, Convergence of Method of Lines approximations to partial differential equations, *Computing*, 33 (1984), 297-313.
- [31] R.A. Weinberg, *The Biology of Cancer*, New York, 2013.